International Journal on Semantic Web and Information Systems
Volume 21 • Issue 1 • January-December 2025

Semantic-Aware Hybrid Deep Learning Model for Brain Tumor Detection and Classification Using Adaptive Feature Extraction and Mask-RCNN

Anil Kumar Mandle
Department of Information Technology, National Institute of Technology Raipur, India

Govind P. Gupta
https://orcid.org/0000-0002-0456-1572
Department of Information Technology, National Institute of Technology Raipur, India

Satya Prakash Sahu
https://orcid.org/0000-0002-9886-9518
Department of Information Technology, National Institute of Technology Raipur, India

Shavi Bansal
https://orcid.org/0009-0009-8699-6884
nsights2Techinfo, India & Center for Interdisciplinary Research, University of Petroleum and Energy Studies (UPES), Dehradun, India

Wadee Alhalabi
https://orcid.org/0000-0002-4505-7268
Department of Computer Science, Immersive Virtual Reality Research Group, King Abdulaziz University, Jeddah, Saudi Arabia

ABSTRACT

A brain tumor is one of the most prevalent causes of cancer death. The best strategy is the timely treatment of brain tumors in their early detection. Magnetic Resonance Imaging (MRI) is a standard non-invasive method to detect brain tumors. For early detection and better patient survival through MRI scans, the diagnosis needs a high level of knowledge in the radiological and neurological domains to identify the cancers. Researchers have suggested various brain cancer detection techniques. However, most existing automatic cancer detection approaches suffer from poor accuracy and low detection rates. This paper proposes a hybrid deep learning (DL) using deep feature extraction and adaptive Mask Region-based Convolutional Neural Networks (Mask-RCNNs) model for brain tumor detection and classification method to overcome these issues. The experimental findings on the benchmark dataset demonstrate that the planned model is highly effective, with 99.64% accuracy, 95.93% precision, 95.39% recall, and 95.67% F1-score.

KEYWORDS

Mask Region-Based Convolution Neural Network, Deep Convolution Neural Network, Brain Tumor, DL, Segmentation, MRI

DOI: 10.4018/IJSWIS.365910

INTRODUCTION

A brain tumor, whether benign or malignant, develops on the brain or skull walls. The growth of skull tumors can stress the brain, resulting in a negative effect on overall health. Timely identification of brain tumors is, therefore, a significant area of investigation within medicinal imaging to identify the most effective treatment options to save a patient's life.

Over the last few decades, medical scientists have discovered more than 120 various forms of brain cancer. These are divided into primary brain cancers, which develop in the brain cells, and secondary brain cancers, which form in the surrounding organs and spread to the brain through blood circulation (Anaraki et al., 2019; Behin et al., 2003). Primary cancers account for approximately 70% of all brain malignancies; secondary cancers account for 30% (Sultan et al., 2019). According to the National Brain Tumor Foundation, about 29,000 instances of primary brain cancers are identified every year in the United States, with 13,000 deaths each year (Akil et al., 2020; Nhi et al., 2022). More than 42,000 people in the United Kingdom die from primary brain cancers each year.

The significant categories of brain cancers include glioma (G), meningioma (M), and pituitary (P). Glioma has the uppermost death and flexibility rates of the different cancers (Maharjan et al., 2020). Low-grade gliomas and high-grade gliomas are two types of gliomas that arise from glial cells in the brain. High-grade gliomas are dangerous, with the patient generally receiving a two-year persistence rate (Qian et al., 2022; Smoll et al., 2013). Meningioma usually forms on the protective tissue layer covering the brain and spinal cord. This type of cancer is often less dangerous and slow in growth (Chu et al., 2022; Louis et al., 2016). Cancers near the pituitary gland, which synthesizes important hormones, are usually benign. However, pituitary cancers affect the functioning of this gland (Masood et al., 2021), threatening the patient's life if not diagnosed in a timely manner.

Various medical imaging modalities can be employed for cancer diagnosis in clinical settings, with the choice depending on the situation and objectives (Chui et al., 2023; Komninos et al., 2004). Non-invasive imaging procedures like computed tomography (CT), MRI, and positron emission tomography (PET) are preferred for early-stage brain tumor detection over invasive methods like biopsies (Ker et al., 2017).

An MRI image is the most effective intra-operative collective imaging process because it does not use hazardous ionizing radiation like x-rays. It provides risk-free, high-quality images of soft tissue, as well as the ability to collect modalities with several parameters, including T1, T1c, T2, and FLAIR. Each modality generates a distinct muscle contrast (Bauer et al., 2013; Chui et al., 2022). The fundamental objective of early therapy for a neurosurgeon is to identify cancer sites correctly. Otherwise, excessive or insufficient excision may cause discomfort or irreversible loss. Manual brain cancer segmentation requires extensive domain knowledge and significant time investment. In addition, it is subject to inter- and intra-variability observations (Masud et al., 2021; Olabarriaga & Smeulders, 2001). Computer-aided diagnosis methods are increasingly utilized as assistive tools to aid in the recognition and classification of brain cancers in MRI scans.

Modern studies illustrate vital advancements in semi-automatic or automatic cancer segmentation techniques. However, research on accurate cancer segmentation remains a challenge (Asa, 1998). First, cancer size, location, and appearance vary from patient to patient (Işın et al., 2016). Second, malignant margins may be abnormal because healthy tissue often fills malignant areas (Goetz et al., 2015). Third, low signal-to-noise ratio or image bias may be caused by MRI acquisition techniques or imaging devices (Mamta & Gupta, 2021; Yao, 2006).

A convolutional neural network (CNN) is a deep learning (DL) model that automatically acquires dense features from training input (Hu et al., 2019). Researchers are, therefore, using DL to segment MRI brain cancers (Litjens et al., 2017). Patch-based techniques input the image into a limited segment of a CNN and categorize each area, improving image quality and identifying connections. The deep CNN (DCNN) is an improved model of the CNN, predicting probability distributions pixel-by-pixel vs. layer-by-layer (Anil et al., 2022; Long et al., 2015). Due to this improvement, DCNN can predict the

entire image in a continuous forward phase. However, the computational time of DL-based algorithms continues to increase due to the presence of convolution layers and required filters.

It is, therefore, crucial to develop a cancer diagnosis and segmentation technique that utilizes less memory and time (Bisht & Vampugani, 2022; Ronneberger et al., 2015). This article presents an automatic detection and classification method for brain cancers in MRI scans. The model uses deep feature extraction with classification via the adaptive mask-region-based CNN (Mask-RCNN) technique. The authors evaluated the developed model using a publicly obtainable brain cancer Figshare dataset to authenticate the performance of the planned technique (Chan, 2017; He et al., 2017). The following are the main contributions of this article:

- The proposed model pre-processing includes median filtering and effective Mask-RCNN used for segmentation and localization of brain tumors.
- The model utilizes advanced deep transfer learning-based models—such as dense network (DenseNet)-41, residual network (ResNet)-18, AlexNet, and GoogLeNet—for effective deep feature extraction.
- The article introduces a novel method integrating hybrid deep feature extraction and adaptive Mask-RCNN for precise brain cancer detection with classification in MRI scans.
- According to extensive evaluations, the result is a higher accuracy, precision, recall, and F1-score performance compared to state-of-the-art approaches.

The remainder of the article is structured as follows. First, the article delivers a comprehensive literature review of related work. The proposed method describes the study's work. The analysis and discussion section presents the study's results and discusses the assessment parameters and outcomes. Finally, the article delivers a conclusion.

RELATED WORK

This section reviews research on brain tumor recognition with classification. ML and DL are commonly used in medical diagnostics, with DL showing promise by directly analyzing raw image data for tasks like segmentation, classification of cancer types, and predicting patient survival rates (Abiwinanda et al., 2019; Afshar et al., 2018; Deepak & Ameer, 2019; Ismael & Abdel-Qader, 2018; Pashaei et al., 2018; Rehman et al., 2020; Sajjad et al., 2019).

Rehman et al. (2020) achieved 98.69% accuracy with CNN and data augmentation for brain cancer classification (glioma, M, and P). Deepak and Ameer (2019) used transfer learning for patient-level brain cancer classification, achieving 98% accuracy. Afshar et al. (2018) used CapsNet for brain cancer classification, achieving 86.50% accuracy. Abiwinanda et al. (2019) developed a CNN-based model, achieving 98.5% training accuracy and 84.29% validation accuracy. Ismael and Abdel-Qader (2018) used Discrete Wavelet Transform and Gabor filters with neural networks, achieving 91.9% accuracy.

Pashaei et al. (2018) introduced a CNN-based model using a customized 3x3 layered setup, achieving 81% accuracy with an Extreme Learning Machine for brain cancer classification. Sajjad et al. (2019) used neural networks for cancer region segmentation in a brain MRI, achieving 90.67% accuracy with noise elimination techniques. Pereira et al. (2018) introduced a CNN for automated G grading using a multi-sequence three-dimensional (3D) MRI. Their study achieved 89.5% accuracy on BRATS-2017 data, enhancing radiologist workflow and treatment accuracy.

Anaraki et al. (2019) used CNN combined with a genetic algorithm to automate brain cancer detection from MRI scans, achieving 90.9% accuracy for glioma and 94.20% for glioma, meningioma, and pituitary cancers. Zhou et al. (2019) converted 3D MRI scans into two-dimensional (2D) slices, using DenseNet-LSTM for classification with 92.13% accuracy. Ahammed Muneer K. V. et al. (2019) improved Wndchrm-based brain cancer classification to 98.25% accuracy using a real clinic dataset.

Banerjee et al. (2019) proposed an innovative methodology for MRI image classification using ConvNet models based on slicing and patching MRI scans, achieving 97% accuracy. Abiwinanda et al. (2019) tested five CNN designs for brain cancer classification, finding simplistic models ineffective. Alanazi et al. [37] introduced a 22-layered CNN architecture, achieving 96.8% accuracy. However, further validation is needed on larger datasets.

Khan et al. (2022) developed a hierarchical DL-based classification technique using MRI scans from the Kaggle dataset, achieving 92.13% accuracy. Further testing is needed for clinical validation. Cheng et al. (2015) achieved 91.28% accuracy using image dilatation and sub-region separation. Albahli et al. (2021) used Faster-RCNN with DenseNet-65, reaching 97.2% accuracy on a Kaggle dataset. Fedorov et al. (2012) reviewed 3D Slicer for developing image study tools in medical research, highlighting its effectiveness and potential future applications. Table 1 discusses related work on brain cancer classification and detection in MRI scans using machine learning and DL methods. Wu et al. (2016) found relationships between big data technologies and the green revolution.

Table 1. Summary of brain cancer detection and classification-related work

Authors	Year	Dataset Training	Dataset	Techniques	Accuracy %	Precision %	Recall %	F1 score %
Swati et al. (2019)	2019	70-80%	CE-MRI images, Figshare (Chan, 2017)	VGG-19	94.82	93.72	94.14	94.82
Toðaçar et al. (2021)	2021	70%	3064 T1-weighted MRI images, Figshare (Chan, 2017)	Attention module & Hyper column technique with Residual block	97.69	94.91	95.51	93.69
Öksüz et al. (2022)	2022	80%	3064 MRI images, Figshare (Chan, 2017)	ResNet-18 for deep feature extractor	97.25	95.30	94.53	94.52
Gumaei et al. (2019)	2019	70%	3064 MRI images, Figshare (Chan, 2017)	GIST descriptor with ELM	94.93	93.92	94.62	93.62
Mandle et al. (2022)	2022	80%	3064 T1-weighted MRI images, Figshare (Chan, 2017)	Kernel-based SVM	98.75	94.42	95.23	95.31
Deepak and Ameer (2019)	2019	80%	3064 T1-weighted MRI images, Figshare (Chan, 2017)	SVM and GoogLeNet	97.10	94.23	93.36	95.12
Pedada et al. (2023)	2023	80%	BraTS 2018 (Chan, 2017)	U-Net	92.81	93.73	93.40	94.58
Huang et al. (2020)	2020	80%	Nanfang Hospital, Guangzhou, China, and General Hospital	CNN-based on complex networks	95.49	94.07	95.20	91.20

continued on following page

Table 1. Continued

Authors	Year	Dataset Training	Dataset	Techniques	Accuracy %	Precision %	Recall %	F1 score %
Rahman and Islam (2023)	2023	80%	3064 T1-weighted MRI images, Figshare (Chan, 2017)	parallel deep CNN	97.60	94.20	94.61	91.70
Kumar and Prince (2023)	2023	80%	Brain MRI images for brain tumor detection (n.d.)	Deep Belief Network	94.12	93.92	95.72	93.42

Swati et al. (2019) proposed VGG16 with VGG19 and AlexNet to identify brain cancers, fine-tuning VGG models block-wise and AlexNet layer-wise. VGG19 achieved the highest accuracy at 94.82%. Huang et al. (2020) designed a DCNN model with an improved activation function, achieving 95.49% accuracy. However, their work had high computational complexity. Gumaei et al. (2019) proposed a normalized extreme learning machine model for feature extraction, achieving 94.233% accuracy.

Toğaçar et al. (2021) proposed a DL-based model, achieving classification accuracies of 98.18% for glioma (G), 96.73% for meningioma (M), and 98.18% for pituitary (P) tumors. Öksüz et al. (2022) pre-trained DL models with a support vector machine (SVM) and k-Nearest Neighbors (k-NN) classifiers, achieving 97.25% accuracy. A Discrete Wavelet Transform-based feature extraction scheme with K-SVM [47] achieved 98.75% accuracy. An improved U-Net model [48] reached 92.8% accuracy on the BraTS dataset. Rahman and Islam (2023) planned a parallel deep CNN model, achieving 97.33% accuracy on the Figshare datasets. Kumar and Prince (2023) used a deep belief network for brain tumor classification, observing 94% accuracy. Wu et al. (2018) discussed the roles and opportunities that information and communication technologies play in pursuing the sustainable development goals.

Most state-of-the-art brain cancer recognition methods focus on benchmark datasets, but face issues like categorization problems and ineffective modern approaches. Despite using automation algorithms and CNN variants, detection hasn't significantly improved. MRI scans present further gaps. This research proposes an end-to-end DL approach using an adaptive Mask-RCNN model for accurate MRI-based recognition and classification.

PROPOSED METHOD

This section details the proposed architecture for brain cancer recognition using an adaptive Mask-RCNN model for segmentation and localization. In addition, advanced transfer learning models—such as DenseNet-41, ResNet-18, AlexNet, and GoogleNet—are utilized for feature extraction with detection and classification. The planned model achieves high accuracy and outperforms state-of-the-art methods in MRI-based cancer detection.

Description of Brain Tumour MRI Dataset

A dataset available on Figshare (Chan, 2017) contains 3,064 T1-weighted MRI scans from 233 patients, including glioma (G), meningioma (M), and pituitary (P) brain cancers. The images are given in sagittal, axial, and coronal planes, with a voxel size of 0.49x0.49 mm^2. The dataset was split 80:20 for training and testing, with 708 glioma, 1426 meningioma, and 930 pituitary cancer

instances. Table 2 summarizes the dataset characteristics and image orientations. Figure 1 shows sample images and ground truth masks.

Table 2. Description of brain cancer MRI images Figshare dataset (Chan, J. 2017)

Cancers	MRI Views	Patients	MR Images	Total Images
Glioma (G)	Horizontal	82	708	209
	transverse			268
	frontal			231
Meningioma (M)	Horizontal	89	1426	494
	transverse			437
	frontal			495
Pituitary (P)	Horizontal	62	930	291
	transverse			319
	frontal			320
Total		**233**	**3064**	**3064**

Figure 1. Sample original images along with ground truth mask

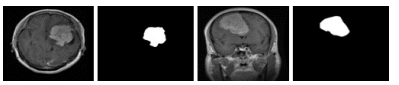

Preprocessing Steps

Preprocessing is crucial in image analysis as it enhances attributes of the images. Skull-stripping techniques remove unwanted regions, speeding up processing and improving accuracy. A median filter is used to reduce noise in brain MRI images, which preserves cancer edge information. The RGB image is converted to grayscale, rotated, and de-noised with the media filter. The edges are identified and the region of interest is cropped. This preprocessing stage ensures high-quality input data for accurate analysis.

Segmentation and Localization Using Adaptive Mask-RCNN

Mask-RCNN is a powerful DL algorithm used for object recognition and instance segmentation in computer vision. It extends Faster RCNNs by adding a branch that generates binary masks for each object instance, enabling pixel-level segmentation. This is crucial for applications requiring precise object boundaries, such as medical imaging. During inference, it accurately detects and segments objects in new images. Figure 3 illustrates this process.

Figure 2. Block data flow diagram of the proposed model

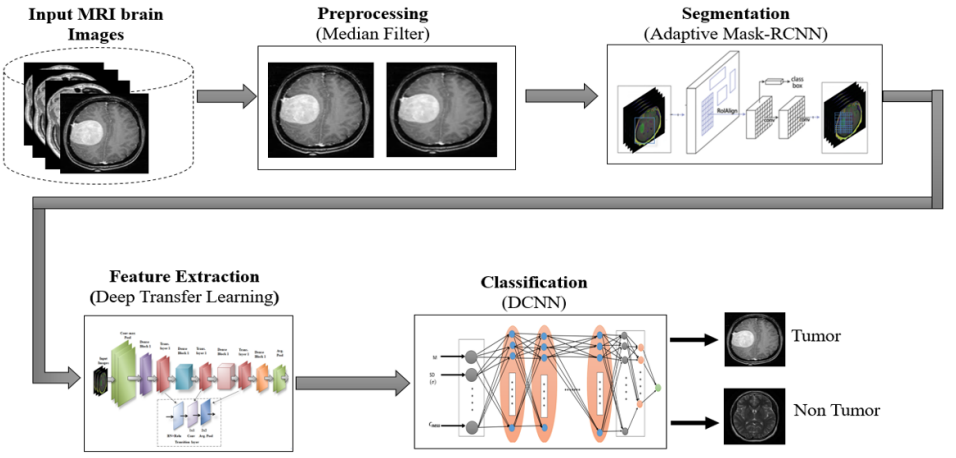

Figure 3. General concept of mask-RCNN architecture

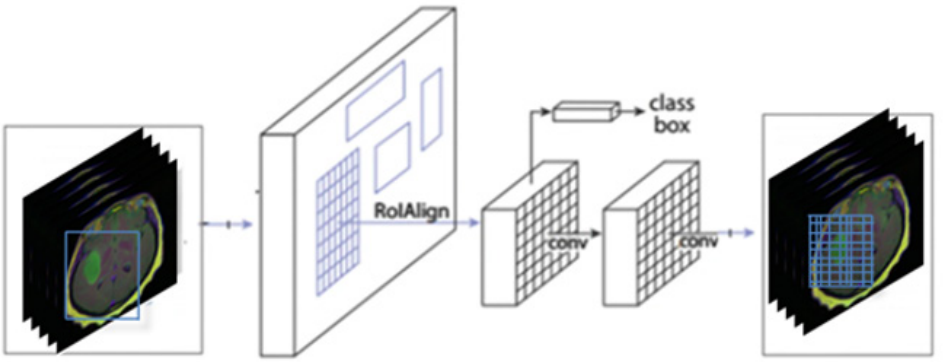

$$\frac{y - y}{y_2 - y}\left(\frac{x_2 - x}{x_2 - x_1}Q_{11} + \frac{x - x_1}{x_2 - x_1}Q_{21}\right) + \frac{y - y_1}{y_2 - y_1}\left(\frac{x_2 - x}{x_2 - x_1}Q_{12} + \frac{x - x_1}{x_2 - x_1}Q_{22}\right) \quad (1)$$

The expression involves the following variables:

- **x and y:** The co-ordinates of the point where the weighted average is being computed.
- x_1, y_1, x_2, y_2**:** The coordinates of the four points Q_{11}, Q_{21}, Q_{12}, and Q_{22}, where $x_1 < x_2$ *and* $y_1 < y_2$.
- $Q_{11}, Q_{21}, Q_{12}, Q_{22}$**:** The values at the four points Q_{11}, Q_{21}, Q_{12}, and Q_{22}.

The classifiers' outputs are subject to post-processing to obtain meaningful outcomes and generate final assessments. The proposed workflow diagram is shown in Figure 4, representing the overall framework of the actual predictable abnormality recognition model. The mask detection approach adopts adaptive Mask-RCNN, which follows the subsequent steps:

- Using "wrapping" instead of "pooling" to identify the regions of interest.

- The proposal regions are identified through the the region proposal network.

Figure 4. Data flow diagram for segmentation through adaptive mask-RCNN

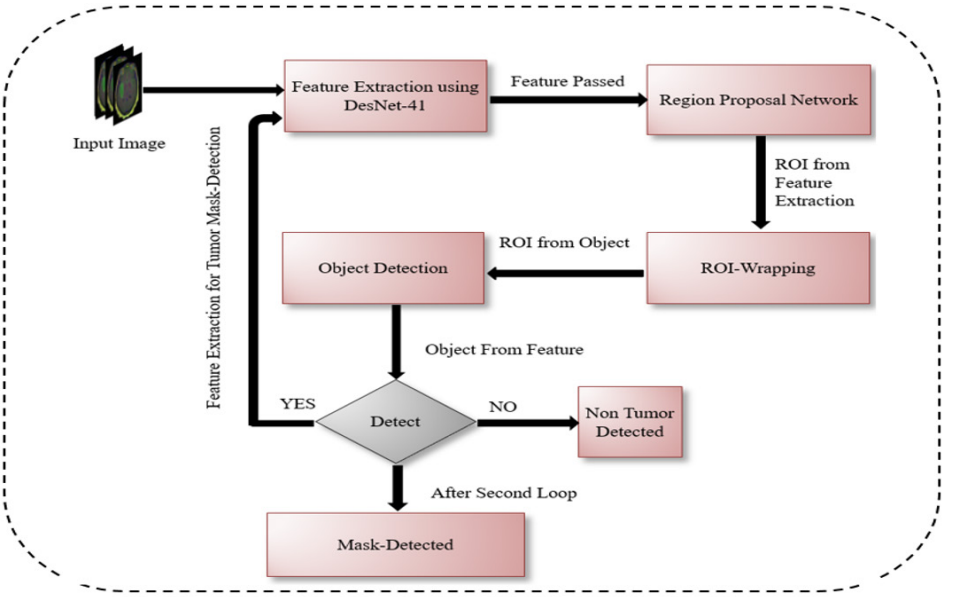

Deep Feature Extraction and Classification

The proposed brain MRI investigation model uses deep feature extraction models like DenseNet-41, ResNet-18, AlexNet, and GoogLeNet. These CNN architectures extract features from preprocessed images. Multiple convolution layers enable accurate feature learning; however, increasing depth poses optimization challenges due to the vanishing gradient issue. The proposed feature extraction techniques are as follows:

- **DenseNet-41 Architecture:** DenseNet-41 is a CNN architecture that utilizes features extraction and classification techniques (see Figure 5). It includes layers of different sizes, each working as follows:
  - **Input Layer:** The network proceeds with an input scan of size 224×224×3.
  - **Convolutional Layer (CL):** The first CL has 64 filters of size 7×7 with a stride-2, reducing the spatial size by a factor-2 and increasing network depth to 64.
  - **Pooling Layer:** The output from the CL goes into 3×3 size with a stride-2 for the max_pooling layer, further halving the spatial size.
  - **Dense Blocks:** DenseNet-41 has four dense blocks with 6, 12, 18, and 6 layers, respectively. Each layer concatenates feature maps from all previous layers in the block.
  - **Transition Layers:** Each pair of dense blocks is separated by a transition layer and a 1×1 CL with a 2×2 average pooling-layer, decreasing channels and spatial size by a factor of 2.
  - **Classification Layer:** The final layer is a global average pooling layer. It has a fully connected layer (FCL) with SoftMax activation, which yields output probabilities for each class.

Figure 5. Architecture of DenseNet-41 model

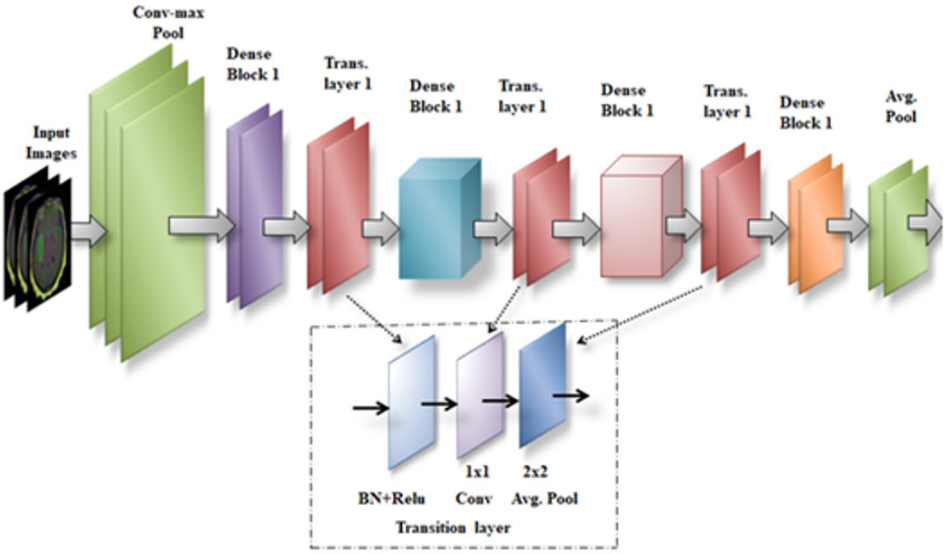

- **ResNet-18 Architecture:** ResNet-18, a CNN model within the ResNet family, features 18 layers. Despite its relative shallowness, it excels in various computer vision tasks like image detection and classification. ResNet-18 uses feature extraction and classification techniques, incorporating layers of different sizes. Each layer performs a specific function (see Figure 6).
  - **Input Layer:** The input network is an RGB scan with sizes of 224×224×3.
  - **CL:** The first layer is a 7×7 CL and stride 2. This is followed with a 3×3 max-pooling and stride 2, as well as four blocks of 2×3×3 CL with 64 filters.
  - **Identity Blocks:** After the first CL, there are four identity blocks that each contain two 3×3 CLs with 64 filters. Each identity block has a shortcut connection that skips the two CLs.
  - **Projection Blocks:** Following the identity blocks, there are four projection blocks that each contain two 3×3 CLs with 128 filters. The first CL in each projection block has a stride of 2, which moderates the spatial sizes of the feature.
  - **Global Average Pooling:** After the last CL, a global average pool layer averages activations of each feature map across spatial sizes.
  - **FCL:** Finally, the output of the global average pooling layer is passed by an FCL with 1,000 nodes, which produces the final classification probabilities for the input image.

Figure 6. Architecture of ResNet-18 model

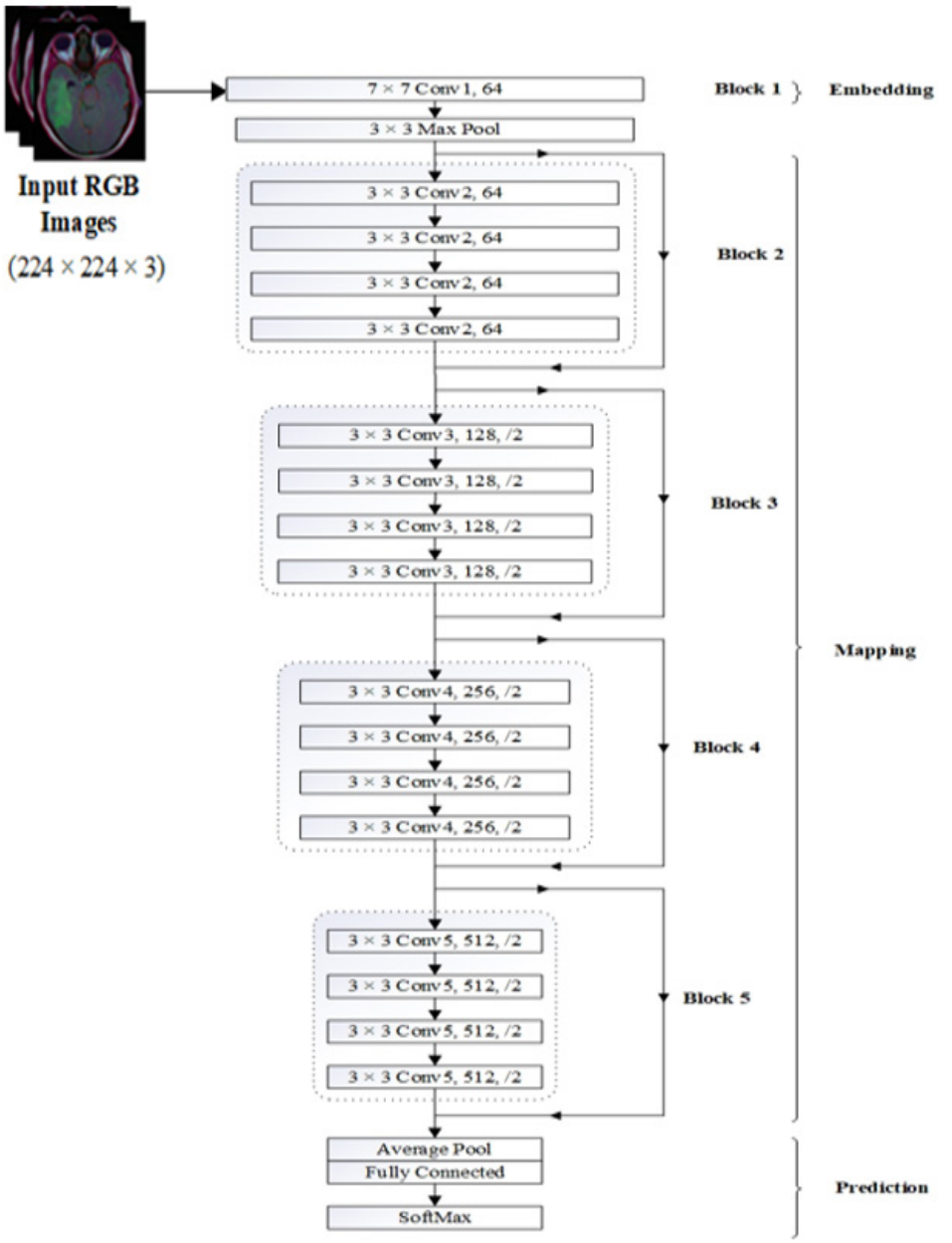

- **AlexNet Architecture:** AlexNet, a CNN model with 18 layers, excels in tasks like image detection and classification. The architecture utilizes feature extraction and classification techniques with various layers, each serving a specific function (see Figure 7).
  - **Input Layer:** A RGB image with dimensions of 227×227×3 is used as the network input.

- **CL:** This layer has filters-96 with size of 11×11 and stride-4. The Rectified Linear Unit (ReLU) activation function and Local Response Normalization are useful to the output layer to level.
- **Max-Pooling Layer:** The output of the first CL is passed through a 3×3 max-pooling layer and stride-2.
- **FCL:** A FCL with 4,096 neurons normalizes and outputs to a ReLU function. This is followed with a dropout layer, which prevents overfitting.

Figure 7. Architecture of AlexNet model

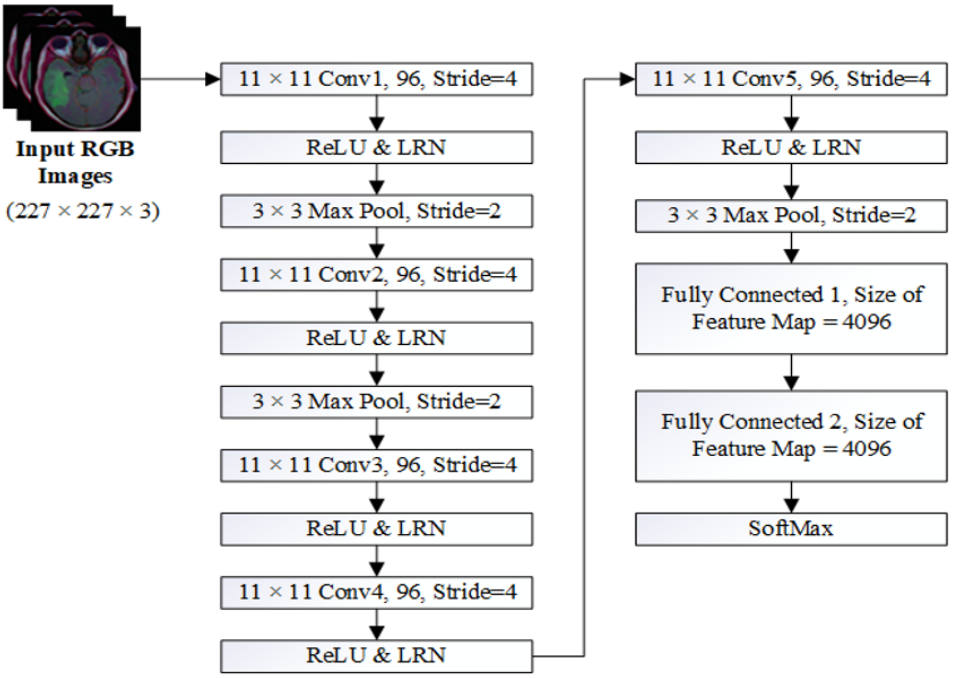

- **GoogleNet Architecture:** GoogleNet is a DCNN architecture excelling in tasks like image detection and classification. It uses feature extraction and classification methods with various layers, each performing specific functions (see Figure 8).
  - **Input Layer:** The layer takes a 224 × 224 × 3 image as input.
  - **CL:** The first CL has 64-filters with a kernel size of 7×7 and a stride-2. The output size of this layer is 112×112×64.
  - **Max Pooling Layer:** The pool size with stride 2 for the first max pooling layer is 3×3. This layer's output measures 56×56×64 pixels.
  - **Inception Module:** The first inception module is composed of four parallel branches of CLs and pooling layers, each with different kernel sizes and numbers of filters. The output size of this layer is 28×28×256.

Figure 8. Architecture of GoogLeNet model

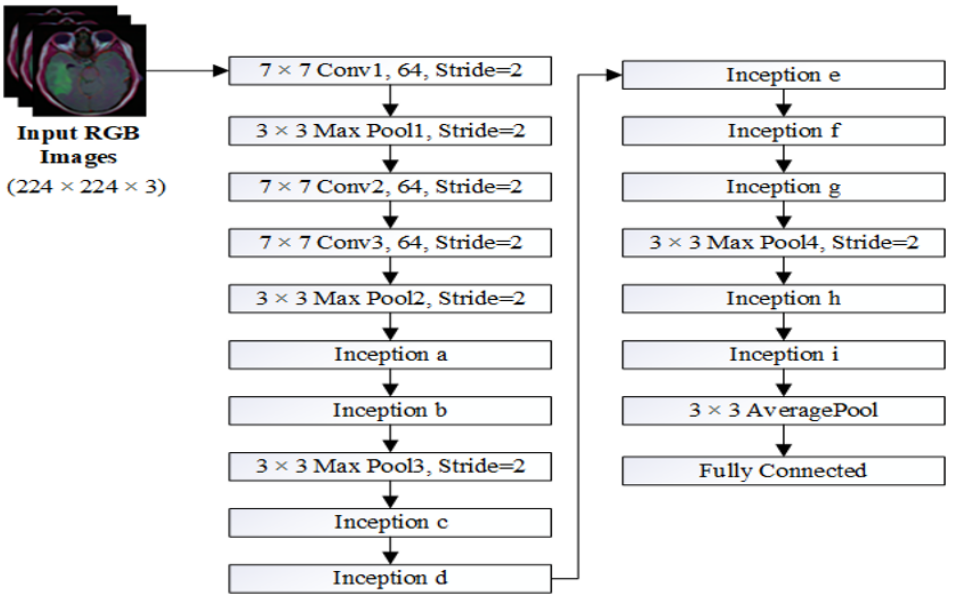

Proposed DCNN Model

This section describes the essential structure of the DCNNs, shown in Figure 9. The DCNN comprises CL, pooling layers, and FCL, each serving specific roles in image processing and analysis tasks.

- **CL:** This uses image filters to remove features—including edges, corners, and textures—from images, producing a feature map.
  - **Pooling Layer:** This layer downsamples feature maps to reduce spatial dimensions and improve model robustness.
  - **Dropout Layer:** This layer prevents overfitting by randomly dropping nodes during training.
  - **FCL:** This layer transforms flattened outputs into class score vectors, indicating class probabilities. Layers can be stacked to create architectures—such as VGG, ResNet, and Inception—with tunable configurations for task-specific optimization.

Figure 9. Proposed DCNN model

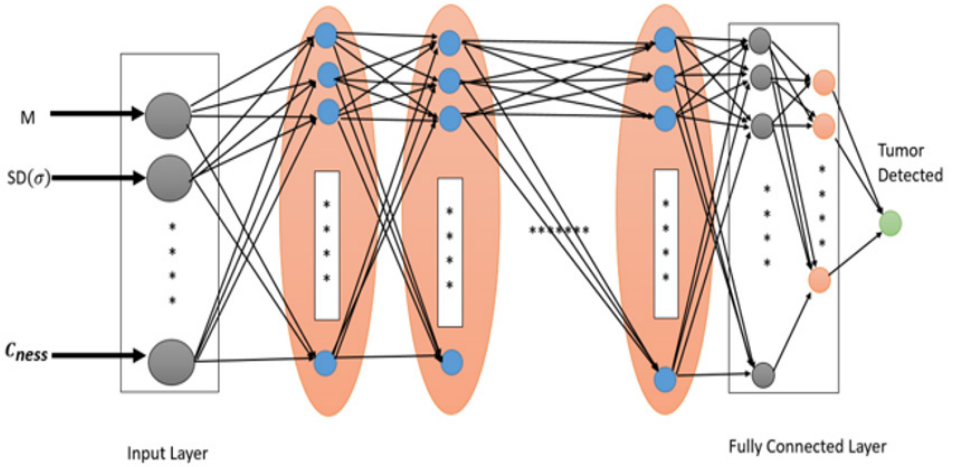

RESULT ANALYSIS AND DISCUSSION

This section presents a comprehensive result analysis of the planned model. It also compares its performance to the latest state-of-art schemes via the Figshare dataset (Chan, 2017). Table 3 lists the parameters used in the proposed adaptive Mask-RCNN-based brain tumor detection model. This work uses a Mask-RCNN architecture by Matter Port Inc. (*Ethereum White Paper*, n.d.).

The Mask-RCNN model uses localization and segmentation. Then, it uses features extraction and classification through DenseNet-41, ResNet-18, AlexNet, and GoogleNet frameworks. In the first analysis, a representative CNN explores the MRI images to categorize meningioma or glioma. Another stage involves transmitting the categorized image via a Mask-RCNN to localize the cancer. A region proposal network track within the adaptive Mask-RCNN model uses COCO net data to construct pre-trained weights for its feature extractor CNN. The second stage results in a border box around the cancer in a 128×128 down-sampled image. With the creative resolution, the boundary boxes are transformed into 512×512 images. Table 3 shows the parameter list used in training the Mask-RCNN-based proposed model.

Table 3. Parameter uses of proposed method for training

Parameters	Optimum Values
No. of CLs	2
No. max-pooling layers	2
No. of FC layer	2
No. of filters	128.96
Size of filter	6.6
Activation Function	ReLU
No. of Epochs	50
Learning rate	0.0001
Momentum	0.90

continued on following page

Table 3. Continued

Parameters	Optimum Values
Mini-batch size	32
Threshold IoU	0.80

Performance investigation of the planned model is associated with several models, including ResNet-50, DenseNet-41, ResNet-18, AlexNet, and GoogLeNet-based adaptive Mask-RCNN. In this article, results showed that DenseNet-41 outperformed ResNet-50 and other models, computing more robust features.

This study visualized the results using several graphical outcomes for conventional Mask-RCNN via Figshare (Chan, 2017) datasets. Despite the common occurrence of discontinuous or unclear borders in MRI scans, DenseNet-41 could accurately locate brain cancers and differentiate them from benign tissues. The CNN-based DenseNet-41 technique effectively overcame size, locality, and shape barriers, resulting in accurate brain cancer segmentation.

To evaluate the performance of the proposed method, this study used a variation of quantitative parameters, including F1-score, recall, and accuracy. The authors suggest that the approach achieved typical accuracy (99.63%) using DenseNet-41 with Figshare (Chan, 2017). However, the DenesNet-41-based adaptive Mask-RCNN method failed to precisely locate brain cancers in restricted images that exhibit visual similarities with healthy tissues (see Figure 10). Therefore, this article recommends a thorough examination and explanation of the findings due to the limitations of the proposed approach.

Figure 10. Efficiency of brain tumor segmentation compared with state-of-the-art techniques

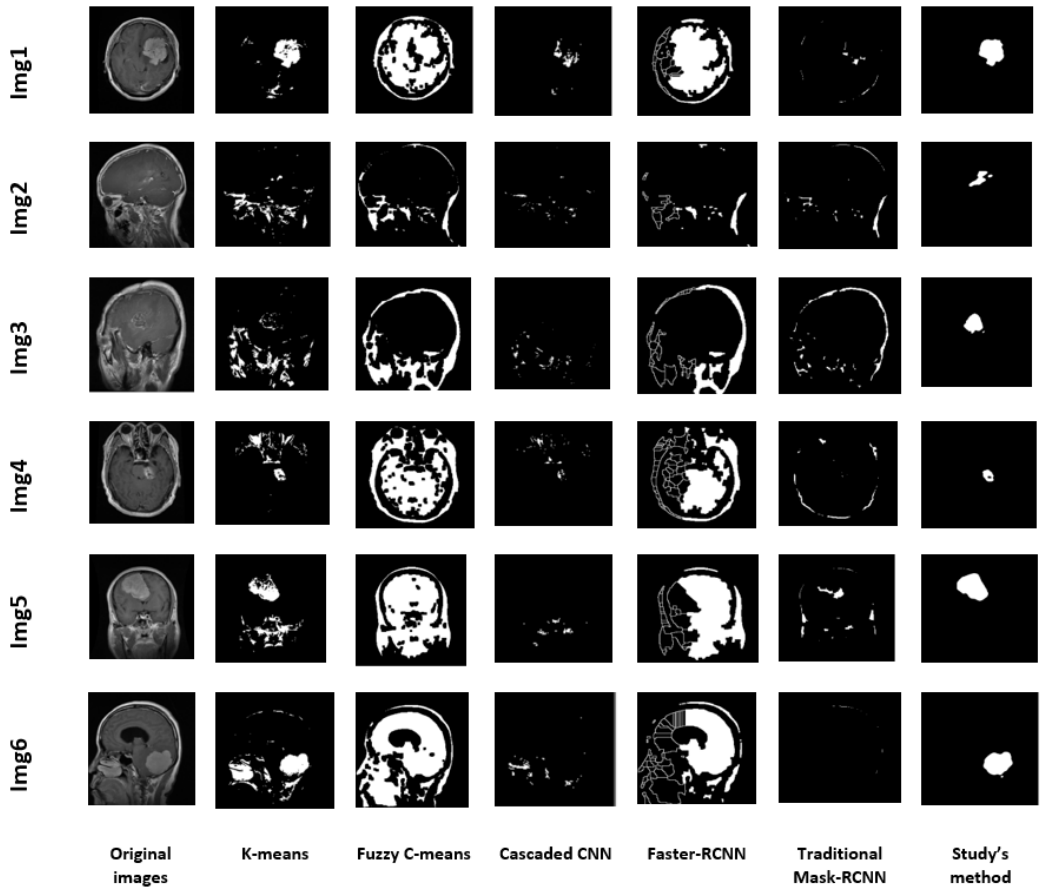

Metrics Evaluation

The following measurement metrics are used to determine the validity of the recommended strategy.

- **Accuracy (A_{cc}):** The accuracy of a model is measured by the number of appropriately predicted labels out of all labels. The calculation of accuracy is as:

$$Accuracy = \frac{TP + TN}{TP + TN + FP + FN} \tag{2}$$

- **Precision (P_c):** Precision measures the section of tumors correctly diagnosed by the model out of all the categorized cancers. It is mathematically defined as:

$$Precision = \frac{TP}{TP + FP} \tag{3}$$

- **Recall (R_c):** This calculates the percentage of cancers within the dataset that were correctly classified. It is mathematically defined as:

$$Recall = \frac{TP}{TP + FN} \tag{4}$$

- **F1-Score (F_s):** F1-score balances calculate the harmonic mean of precision with recall.

$$F1 - score = 2 \times \frac{Precision \times Recall}{Precision + Recall} \tag{5}$$

Here, the assignment is to categorize whether a tissue sample is cancerous. They are listed as true positive (cancer samples that are correctly classified as cancerous), true negative (healthy tissue samples that are correctly classified as non-cancerous), false positive (healthy tissue samples that are incorrectly classified as cancerous), and false negative (cancer samples that are incorrectly classified as non-cancerous).

Figure 11 illustrates the confusion matrix of the proposed model. It is displayed through features after the training of the DL model and employed to observe overfitting issues impacting misclassifications. Overfitting may be prevented through data augmentation and the use of the right number of training iterations. In the proposed model, the overfitting issue is resolved using dropout regularization and batch normalization-based techniques.

Figure 11. Confusion matrix glioma (G), meningioma (M), and pituitary (P)

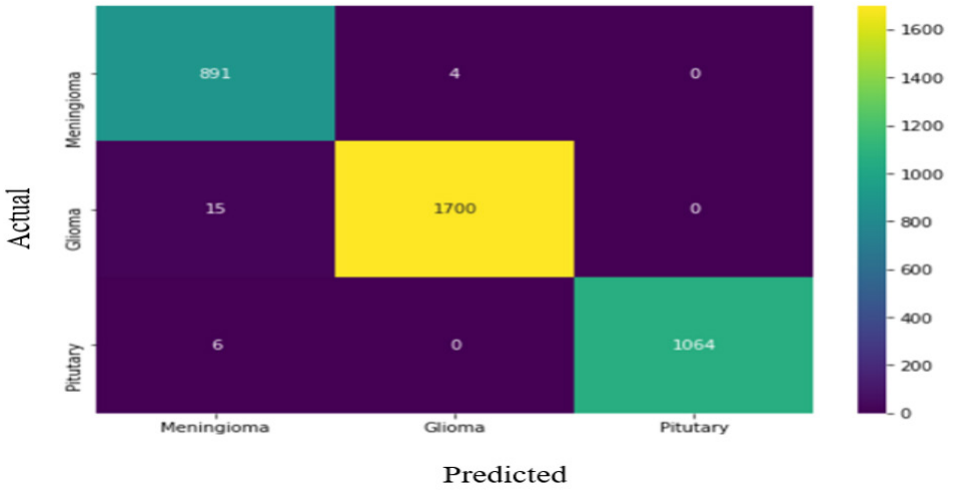

Table 4 lists the comparative results of the proposed segmentation technique with state-of-the-art techniques like Cascaded-CNN (Sobhaninia et al., 2020), Faster RCNN (Gunasekara et al., 2021), Fuzzy-C-Means (Sheela & Suganthi, 2020), Traditional Mask-RCNN (Masood et al., 2021), and K-Means (Öksüz et al., 2022). It is observed from the experiments that the proposed adaptive Mask R-CCN has achieved 97.3% accuracy and outperforms existing methods. This is because the planned adaptive Mask-RCCN-based model generalizes the model behavior by utilizing the deep feature learning. Figure 10 presents the visualization results of the proposed segmentation technique associated with state-of-the-art methods.

Table 4. Segmentation techniques compared with existing methods

Technique	Evaluation Metrics		
	Mean IoU	DSC	Accuracy
K-Means (Toðaçar et al., 2021)	0.940	0.941	0.945
Fuzzy-C-Means (Sheela & Suganthi, 2020)	0.946	0.665	0.910
Cascaded CNN (Sobhaninia et al., 2020)	0.907	0.800	0.943
Faster RCNN [55]	0.924	0.920	0.946
Traditional Mask-RCNN (Gunasekara et al., 2021)	0.950	0.950	0.951
Proposed [Adaptive Mask-RCNN]	0.957	0.959	0.973

Performance Evaluation of the Proposed Approach With State-of-the-Art Approaches

This section assesses planned technique classification performance compared to studies that used a similar dataset (Chan, 2017). It is observed from the result analysis that the proposed method outperforms other methods in terms of accuracy. The accuracy achieved by the proposed method is 99.6%. Figure 12 demonstrates the proportional graphical performance of accuracy (A_{cc}), precision (P_c), recall (R_c), and F1-score *(F_s)* between the proposed technique and state-of-the-art techniques.

Figure 12. Performance analysis of proposed method compared to state-of-the-art methods

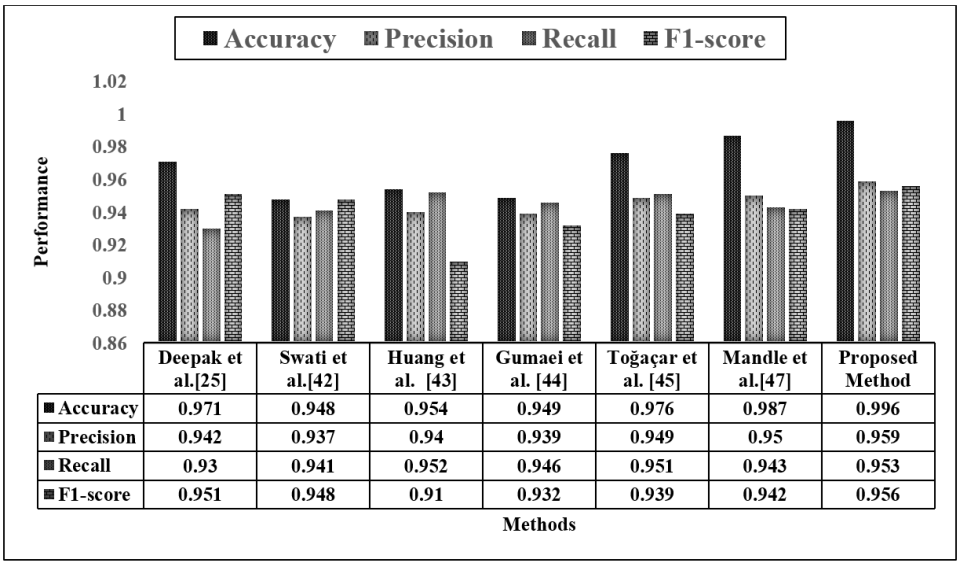

	Deepak et al.[25]	Swati et al.[42]	Huang et al. [43]	Gumaei et al. [44]	Toğaçar et al. [45]	Mandle et al.[47]	Proposed Method
Accuracy	0.971	0.948	0.954	0.949	0.976	0.987	0.996
Precision	0.942	0.937	0.94	0.939	0.949	0.95	0.959
Recall	0.93	0.941	0.952	0.946	0.951	0.943	0.953
F1-score	0.951	0.948	0.91	0.932	0.939	0.942	0.956

RCNN approaches have the disadvantage of taking a long time to train because they produce approximately 2,000 region proposals for categorization at random. Moreover, the fixed selective search technique used in the region proposal generation stage does not involve a learning process, leading to incorrect region suggestions.

Compared to Faster RCNN, RCNN is easier to train and has lower overhead. Due to its dense networks, the DenseNet-41-based technique planned in this work is more efficient than ResNet-50,

resulting in a more precise evaluation of image features. The Mask-RCNN based on DenseNet-41 is also more computationally effective due to its limited parameter number. The complex nature of cancers, including overlapping borders and MRI artifacts, can lead to misclassification of cancer types in the overall image result when using the techniques mentioned in previous studies (Kumar & Prince, 2023; Pedada et al., 2023; Rahman & Islam, 2023). These methods rely on less selective and robust hand-crafted features (*Brain MRI images for brain tumor detection*, n.d.).

While a similar strategy has been proposed in this article, it employs the hyper column method, which is computationally expensive and prone to overfitting. In contrast, the authors' suggested approach utilizes deep features that are more distinctive and consistent (*Ethereum White Paper*, n.d.). Additionally, a CNN model that employs region-based techniques to emphasize the cancer region of interest before performing analysis or classification has yielded improved accuracy in cancer detection.

CONCLUSIONS AND FUTURE SCOPE

This article presented an adaptive Mask-RCNN and DenseNet-41 backbones-based DL technique for the accurate identification of brain tumors in MRI images. DenseNet-41, ResNet-18, AlexNet, and GoogLeNet-based adaptive Mask-RCNN produced higher detection and classification results compared with existing methods, resulting in improved image feature computations. Performance analysis demonstrates that the planned model identifies the cancer region more precisely. Thus, it may be a novel automated investigative tool. The proposed adaptive Mask-RCNN method can calculate deep features through operational illustrations of brain cancers, which is higher than state-of-the-art techniques.

The experimental findings on the benchmark dataset validated that the proposed model is effective, with 99.64% accuracy, 95.93% precision, 95.39% recall, and 95.67% F1-score. Though the planned model performs well in terms of accuracy, regarding clinical practices, the proposed model needs to be tested with a more diversified dataset of different age groups.

The authors plan to perform experiments with the proposed model in other applications of medical imaging, including eye infection identification, finger skin identification, skin cancer recognition, and COVID recognition. In addition, the authors aim to use an explainable artificial intelligence model to perform a deep performance analysis of the proposed hybrid model.

COMPETING INTERESTS

The authors of this publication declare there are no competing interests.

FUNDING STATEMENT

This research work was funded by Institutional Fund Projects under grant no. (IFPIP-1119-611-1443). Therefore, the authors gratefully acknowledge technical and financial support from the Ministry of Education and Deanship of Scientific Research (DSR), King Abdulaziz University (KAU), Jeddah, Saudi Arabia.

PROCESS DATES

December 16, 2024
Received: October 21, 2024, Revision: November 24, 2024, Accepted: November 25, 2024

CORRESPONDING AUTHOR

Correspondence should be addressed to Shavi Bansal (India, shavi@insights2techinfo.com)

REFERENCES

Abiwinanda, N., Hanif, M., Hesaputra, S. T., Handayani, A., & Mengko, T. R. (2019). Brain tumor classification using convolutional neural network. In L. Lhotska, L. Sukupova, I. Lacković, & G. S. Ibbott (Eds.), *World Congress on Medical Physics and Biomedical Engineering 2018* (Vol. 68/1, pp. 183–189). Springer Nature Singapore. DOI: 10.1007/978-981-10-9035-6_33

Afshar, P., Mohammadi, A., & Plataniotis, K. N. (2018). *Brain tumor type classification via capsule networks. 25th IEEE International Conference on Image Processing (ICIP)*. IEEE., https://ieeexplore.ieee.org/abstract/document/8451379/

Ahammed Muneer, K. V., & Rajendran, V. R. (2019). Glioma tumor grade identification using artificial intelligent techniques. *Journal of Medical Systems*, *43*(5), 113. DOI: 10.1007/s10916-019-1228-2 PMID: 30900029

Akil, M., Saouli, R., & Kachouri, R. (2020). Fully automatic brain tumor segmentation with deep learning-based selective attention using overlapping patches and multi-class weighted cross-entropy. [Alanazi et al.]. *Medical Image Analysis*, *63*, 101692. DOI: 10.1016/j.media.2020.101692 PMID: 32417714

Albahli, S., Nazir, T., Irtaza, A., & Javed, A. (2021). Recognition and detection of diabetic retinopathy using Densenet-65 Based Faster-RCNN. *Computers, Materials & Continua*, *67*(2), 1333–1351. DOI: 10.32604/cmc.2021.014691

Anaraki, A. K., Ayati, M., & Kazemi, F. (2019). Magnetic resonance imaging-based brain tumor grades classification and grading via convolutional neural networks and genetic algorithms. *Biocybernetics and Biomedical Engineering*, *39*(1), 63–74. DOI: 10.1016/j.bbe.2018.10.004

Anil, B. C., Dayananda, P., Nethravathi, B., & Raisinghani, M. S. (2022). Efficient local cloud-based solution for liver cancer detection using deep learning. *International Journal of Cloud Applications and Computing*, *12*(1), 1–13. DOI: 10.4018/IJCAC.2022010109

Asa, S. L. (1998). *Tumors of the pituitary gland*. American Registry of Pathology. https://books.google.com/books?hl=en&lr=&id=v2BsAAAAMAAJ&oi=fnd&pg=PA1&dq=Asa,+S.+L.+(1998).%C2%A0Cancers+of+the+pituitary+gland.+Amer+Registry+of+Pathology&ots=NvV7-hvNX0&sig=KzkwrNkJoMots7kAiSCmQUSVrhI

Banerjee, S., Mitra, S., Masulli, F., & Rovetta, S. (2019). *Deep radiomics for brain tumor detection and classification from multi-sequence MRI* (arXiv:1903.09240). arXiv. http://arxiv.org/abs/1903.09240

Bauer, S., Wiest, R., Nolte, L.-P., & Reyes, M. (2013). A survey of MRI-based medical image analysis for brain tumor studies. *Physics in Medicine and Biology*, *58*(13), R97–R129. DOI: 10.1088/0031-9155/58/13/R97 PMID: 23743802

Behin, A., Hoang-Xuan, K., Carpentier, A. F., & Delattre, J.-Y. (2003). Primary brain tumours in adults. *Lancet*, *361*(9354), 323–331. DOI: 10.1016/S0140-6736(03)12328-8 PMID: 12559880

Bisht, J., & Vampugani, V. S. (2022). Load and cost-aware min-min workflow scheduling algorithm for heterogeneous resources in fog, cloud, and edge scenarios. *International Journal of Cloud Applications and Computing*, *12*(1), 1–20. DOI: 10.4018/IJCAC.2022010105

Brain MRI images for brain tumor detection. (n.d.). Kaggle. https://www.kaggle.com/navoneel/brain-mri-images-for-brain-tumor-detection

Chan, J. (2017). *Brain tumor dataset* [Dataset]. figshare. DOI: 10.6084/m9.figshare.1512427.v5

Cheng, J., Huang, W., Cao, S., Yang, R., Yang, W., Yun, Z., Wang, Z., & Feng, Q. (2015). Enhanced performance of brain tumor classification via tumor region augmentation and partition. *PLoS One*, *10*(10), e0140381. DOI: 10.1371/journal.pone.0140381 PMID: 26447861

Chu, J., Zhao, X., Song, D., Li, W., Zhang, S., Li, X., & Liu, A. A. (2022). Improved semantic representation learning by multiple clustering for image-based 3D model retrieval. *International Journal on Semantic Web and Information Systems*, *18*(1), 1–20. DOI: 10.4018/IJSWIS.297033

Chui, K. T., Gupta, B. B., Chi, H. R., Arya, V., Alhalabi, W., Ruiz, M. T., & Shen, C. W. (2022). Transfer learning-based multi-scale denoising convolutional neural network for prostate cancer detection. *Cancers (Basel)*, *14*(15), 3687. DOI: 10.3390/cancers14153687 PMID: 35954350

Chui, K. T., Gupta, B. B., Jhaveri, R. H., Chi, H. R., Arya, V., Almomani, A., & Nauman, A. (2023). Multiround transfer learning and modified generative adversarial network for lung cancer detection. *International Journal of Intelligent Systems*, *2023*(1), 6376275. DOI: 10.1155/2023/6376275

Deepak, S., & Ameer, P. M. (2019). Brain tumor classification using deep CNN features via transfer learning. *Computers in Biology and Medicine*, *111*, 103345. DOI: 10.1016/j.compbiomed.2019.103345 PMID: 31279167

Ethereum White Paper. (n.d.). GitHub. https://github.com/ethereum/wiki

Fedorov, A., Beichel, R., Kalpathy-Cramer, J., Finet, J., Fillion-Robin, J.-C., Pujol, S., Bauer, C., Jennings, D., Fennessy, F., Sonka, M., Buatti, J., Aylward, S., Miller, J. V., Pieper, S., & Kikinis, R. (2012). 3D Slicer as an image computing platform for the quantitative imaging network. *Magnetic Resonance Imaging*, *30*(9), 1323–1341. DOI: 10.1016/j.mri.2012.05.001 PMID: 22770690

Goetz, M., Weber, C., Binczyk, F., Polanska, J., Tarnawski, R., Bobek-Billewicz, B., Koethe, U., Kleesiek, J., Stieltjes, B., & Maier-Hein, K. H. (2015). DALSA: Domain adaptation for supervised learning from sparsely annotated MR images. *IEEE Transactions on Medical Imaging*, *35*(1), 184–196. DOI: 10.1109/TMI.2015.2463078 PMID: 26259241

Gumaei, A., Hassan, M. M., Hassan, M. R., Alelaiwi, A., & Fortino, G. (2019). A hybrid feature extraction method with regularized extreme learning machine for brain tumor classification. *IEEE Access : Practical Innovations, Open Solutions*, *7*, 36266–36273. DOI: 10.1109/ACCESS.2019.2904145

Gunasekara, S. R., Kaldera, H. N. T. K., & Dissanayake, M. B. (2021). A systematic approach for MRI brain tumor localization and segmentation using deep learning and active contouring. *Journal of Healthcare Engineering*, *2021*, 1–13. DOI: 10.1155/2021/6695108 PMID: 33777346

He, K., Gkioxari, G., Dollár, P., & Girshick, R. (2017). Mask R-CNN. *Proceedings of the IEEE International Conference on Computer Vision* (pp. 2961–2969). https://openaccess.thecvf.com/content_iccv_2017/html/He_Mask_R-CNN_ICCV_2017_paper.html

Hu, K., Gan, Q., Zhang, Y., Deng, S., Xiao, F., Huang, W., Cao, C., & Gao, X. (2019). Brain tumor segmentation using multi-cascaded convolutional neural networks and conditional random field. *IEEE Access : Practical Innovations, Open Solutions*, *7*, 92615–92629. DOI: 10.1109/ACCESS.2019.2927433

Huang, Z., Du, X., Chen, L., Li, Y., Liu, M., Chou, Y., & Jin, L. (2020). Convolutional neural network based on complex networks for brain tumor image classification with a modified activation function. *IEEE Access : Practical Innovations, Open Solutions*, *8*, 89281–89290. DOI: 10.1109/ACCESS.2020.2993618

Işın, A., Direkoğlu, C., & Şah, M. (2016). Review of MRI-based brain tumor image segmentation using deep learning methods. *Procedia Computer Science*, *102*, 317–324. DOI: 10.1016/j.procs.2016.09.407

Ismael, M. R., & Abdel-Qader, I. (2018). *Brain tumor classification via statistical features and back-propagation neural network. 2018 IEEE International Conference on Electro/Information Technology (EIT) (pp. 0252–0257)*. IEEE., https://ieeexplore.ieee.org/abstract/document/8500308/

Ker, J., Wang, L., Rao, J., & Lim, T. (2017). Deep learning applications in medical image analysis. *IEEE Access: Practical Innovations, Open Solutions*, *6*, 9375–9389. DOI: 10.1109/ACCESS.2017.2788044

Khan, A. H., Abbas, S., Khan, M. A., Farooq, U., Khan, W. A., Siddiqui, S. Y., & Ahmad, A. (2022). Intelligent model for brain tumor identification using deep learning. *Applied Computational Intelligence and Soft Computing*, *2022*, 1–10. DOI: 10.1155/2022/8104054

Komninos, J., Vlassopoulou, V., Protopapa, D., Korfias, S., Kontogeorgos, G., Sakas, D. E., & Thalassinos, N. C. (2004). Tumors metastatic to the pituitary gland: Case report and literature review. *The Journal of Clinical Endocrinology and Metabolism*, *89*(2), 574–580. DOI: 10.1210/jc.2003-030395 PMID: 14764764

Kumar, V. V., & Prince, P. G. K. (2023). Deep belief network Assisted quadratic logit boost classifier for brain tumor detection using MR images. *Biomedical Signal Processing and Control*, *81*, 104415. DOI: 10.1016/j.bspc.2022.104415

Litjens, G., Kooi, T., Bejnordi, B. E., Setio, A. A. A., Ciompi, F., Ghafoorian, M., Van Der Laak, J. A., Van Ginneken, B., & Sánchez, C. I. (2017). A survey on deep learning in medical image analysis. *Medical Image Analysis*, *42*, 60–88. DOI: 10.1016/j.media.2017.07.005 PMID: 28778026

Long, J., Shelhamer, E., & Darrell, T. (2015). Fully convolutional networks for semantic segmentation. *Proceedings of the IEEE Conference on Computer Vision and Pattern Recognition* (pp. 3431–3440). https://openaccess.thecvf.com/content_cvpr_2015/html/Long_Fully_Convolutional_Networks_2015_CVPR_paper.html

Louis, D. N., Perry, A., Reifenberger, G., Von Deimling, A., Figarella-Branger, D., Cavenee, W. K., Ohgaki, H., Wiestler, O. D., Kleihues, P., & Ellison, D. W. (2016). The 2016 World Health Organization Classification of Tumors of the Central Nervous System: A summary. *Acta Neuropathologica*, *131*(6), 803–820. DOI: 10.1007/s00401-016-1545-1 PMID: 27157931

Maharjan, S., Alsadoon, A., Prasad, P. W. C., Al-Dalain, T., & Alsadoon, O. H. (2020). A novel enhanced softmax loss function for brain tumour detection using deep learning. *Journal of Neuroscience Methods*, *330*, 108520. DOI: 10.1016/j.jneumeth.2019.108520 PMID: 31734325

Mamta, & Gupta, B. (2021). An attribute-based keyword search for m-health networks. *Journal of Computer Virology and Hacking Techniques, 17*(1), 21–36.

Mandle, A. K., Sahu, S. P., & Gupta, G. (2022). Brain tumor segmentation and classification in MRI using clustering and kernel-based SVM. *Biomedical & Pharmacology Journal*, *15*(2), 699–716. DOI: 10.13005/bpj/2409

Masood, M., Nazir, T., Nawaz, M., Mehmood, A., Rashid, J., Kwon, H.-Y., Mahmood, T., & Hussain, A. (2021). A novel deep learning method for recognition and classification of brain tumors from MRI images. *Diagnostics (Basel)*, *11*(5), 744. DOI: 10.3390/diagnostics11050744 PMID: 33919358

Masud, M., Hossain, M. S., Alhumyani, H., Alshamrani, S. S., Cheikhrouhou, O., Ibrahim, S., Muhammad, G., Rashed, A. E. E., & Gupta, B. B. (2021). Pre-trained convolutional neural networks for breast cancer detection using ultrasound images. *ACM Transactions on Internet Technology*, *21*(4), 1–17. DOI: 10.1145/3418355

Nhi, N. T. U., & Le, T. M.Thanh The Van. (2022). A model of semantic-based image retrieval using C-tree and neighbor graph. *International Journal on Semantic Web and Information Systems*, *18*(1), 1–23. DOI: 10.4018/IJSWIS.295551

Öksüz, C., Urhan, O., & Güllü, M. K. (2022). Brain tumor classification using the fused features extracted from expanded tumor region. *Biomedical Signal Processing and Control*, *72*, 103356. DOI: 10.1016/j.bspc.2021.103356

Olabarriaga, S. D., & Smeulders, A. W. (2001). Interaction in the segmentation of medical images: A survey. *Medical Image Analysis*, *5*(2), 127–142. DOI: 10.1016/S1361-8415(00)00041-4 PMID: 11516707

Pashaei, A., Sajedi, H., & Jazayeri, N. (2018). *Brain tumor classification via convolutional neural network and extreme learning machines. 2018 8th International Conference on Computer and Knowledge Engineering*. ICCKE., https://ieeexplore.ieee.org/abstract/document/8566571/

Pedada, K. R., Rao, B., Patro, K. K., Allam, J. P., Jamjoom, M. M., & Samee, N. A. (2023). A novel approach for brain tumour detection using deep learning based technique. *Biomedical Signal Processing and Control*, *82*, 104549. DOI: 10.1016/j.bspc.2022.104549

Pereira, S., Meier, R., Alves, V., Reyes, M., & Silva, C. A. (2018). Automatic brain tumor grading from MRI data using convolutional neural networks and quality assessment. In D. Stoyanov, Z. Taylor, S. M. Kia, I. Oguz, M. Reyes, A. Martel, L. Maier-Hein, A. F. Marquand, E. Duchesnay, T. Löfstedt, B. Landman, M. J. Cardoso, C. A. Silva, S. Pereira, & R. Meier (Eds.), *Understanding and interpreting machine learning in medical image computing applications* (Vol. 11038, pp. 106–114). Springer International Publishing. DOI: 10.1007/978-3-030-02628-8_12

Qian, W., Li, H., & Mu, H. (2022). Circular LBP prior-based enhanced GAN for image style transfer. *International Journal on Semantic Web and Information Systems*, *18*(2), 1–15. DOI: 10.4018/IJSWIS.315601

Rahman, T., & Islam, M. S. (2023). MRI brain tumor detection and classification using parallel deep convolutional neural networks. *Measurement. Sensors*, *26*, 100694. DOI: 10.1016/j.measen.2023.100694

Rehman, A., Naz, S., Razzak, M. I., Akram, F., & Imran, M. (2020). A deep learning-based framework for automatic brain tumors classification using transfer learning. *Circuits, Systems, and Signal Processing*, *39*(2), 757–775. DOI: 10.1007/s00034-019-01246-3

Ronneberger, O., Fischer, P., & Brox, T. (2015). U-Net: Convolutional networks for biomedical image segmentation. In Navab, N., Hornegger, J., Wells, W. M., & Frangi, A. F. (Eds.), *Vol. 9351*, pp. 234–241). Medical image computing and computer-assisted intervention. Springer International Publishing., DOI: 10.1007/978-3-319-24574-4_28

Sajjad, M., Khan, S., Muhammad, K., Wu, W., Ullah, A., & Baik, S. W. (2019). Multi-grade brain tumor classification using deep CNN with extensive data augmentation. *Journal of Computational Science*, *30*, 174–182. DOI: 10.1016/j.jocs.2018.12.003

Sheela, C. J. J., & Suganthi, G. (2020). Brain tumor segmentation with radius contraction and expansion based initial contour detection for active contour model. *Multimedia Tools and Applications*, *79*(33–34), 23793–23819. DOI: 10.1007/s11042-020-09006-1

Smoll, N. R., Schaller, K., & Gautschi, O. P. (2013). Long-term survival of patients with glioblastoma multiforme (GBM). *Journal of Clinical Neuroscience*, *20*(5), 670–675. DOI: 10.1016/j.jocn.2012.05.040 PMID: 23352352

Sobhaninia, Z., Rezaei, S., Karimi, N., Emami, A., & Samavi, S. (2020). *Brain tumor segmentation by cascaded deep neural networks using multiple image scales. 2020 28th Iranian Conference on Electrical Engineering*. ICEE., https://ieeexplore.ieee.org/abstract/document/9260876/

Sultan, H. H., Salem, N. M., & Al-Atabany, W. (2019). Multi-classification of brain tumor images using deep neural network. *IEEE Access : Practical Innovations, Open Solutions*, *7*, 69215–69225. DOI: 10.1109/ACCESS.2019.2919122

Swati, Z. N. K., Zhao, Q., Kabir, M., Ali, F., Ali, Z., Ahmed, S., & Lu, J. (2019). Brain tumor classification for MR images using transfer learning and fine-tuning. *Computerized Medical Imaging and Graphics*, *75*, 34–46. DOI: 10.1016/j.compmedimag.2019.05.001 PMID: 31150950

Toğaçar, M., Ergen, B., & Cömert, Z. (2021). Tumor type detection in brain MR images of the deep model developed using hypercolumn technique, attention modules, and residual blocks. *Medical & Biological Engineering & Computing*, *59*(1), 57–70. DOI: 10.1007/s11517-020-02290-x PMID: 33222016

Wu, J., Guo, S., Huang, H., Liu, W., & Xiang, Y. (2018). Information and communications technologies for sustainable development goals: State-of-the-art, needs and perspectives. *IEEE Communications Surveys and Tutorials*, *20*(3), 2389–2406. DOI: 10.1109/COMST.2018.2812301

Wu, J., Guo, S., Li, J., & Zeng, D. (2016). Big data meet green challenges: Big data toward green applications. *IEEE Systems Journal*, *10*(3), 888–900. DOI: 10.1109/JSYST.2016.2550530

Yao, J. (2006). Image processing in tumor imaging. *New Techniques in Oncologic Imaging*, 79–102.

Zhou, Y., Li, Z., Zhu, H., Chen, C., Gao, M., Xu, K., & Xu, J. (2019). Holistic brain tumor screening and classification based on DenseNet and recurrent neural network. In Crimi, A., Bakas, S., Kuijf, H., Keyvan, F., Reyes, M., & Van Walsum, T. (Eds.), *Brainlesion: Glioma, multiple sclerosis, stroke and traumatic brain injuries* (*Vol. 11383*, pp. 208–217). Springer International Publishing., DOI: 10.1007/978-3-030-11723-8_21